EBioMedicine 14 (2016) 44–54

Contents lists available at ScienceDirect

EBioMedicine

journal homepage: www.ebiomedicine.com

Research Paper

# Preclinical Efficacy and Safety Assessment of Artemisinin-Chemotherapeutic Agent Conjugates for Ovarian Cancer

Xiaoguang Li [a,b,1], Yu Zhou [c,1], Yanling Liu [b], Xu Zhang [c], Tao Chen [b], Kerong Chen [c], Qian Ba [a,b], Jingquan Li [a,b], Hong Liu [c,**], Hui Wang [a,b,d,*]

[a] School of Public health, Shanghai Jiao Tong University School of Medicine, Shanghai, China
[b] Key Laboratory of Food Safety Research, Institute for Nutritional Sciences, Shanghai Institutes for Biological Sciences, Chinese Academy of Sciences, Shanghai 200031, China
[c] Key Laboratory of Receptor Research, Shanghai Institute of Materia Medica, Chinese Academy of Sciences, Shanghai, China
[d] Key Laboratory of Food Safety Risk Assessment, Ministry of Health, Beijing, China

ARTICLE INFO

*Article history:*
Received 7 June 2016
Received in revised form 21 November 2016
Accepted 21 November 2016
Available online 23 November 2016

*Keywords:*
Dihydroartemisinin
Drug conjugates
Cell cycle
Apoptosis
Metastasis
Ovarian cancer

ABSTRACT

Artemisinin (ARS) and its derivatives, which are clinically used antimalarial agents, have shown antitumor activities. Their therapeutic potencies, however, are limited by their low solubility and poor bioavailability. Here, through a pharmacophore hybridization strategy, we synthesized ARS-drug conjugates, in which the marketed chemotherapeutic agents chlorambucil, melphalan, flutamide, aminoglutethimide, and doxifluridine, were separately bonded to Dihydroartemisinin (DHA) through various linkages. Of these, the artemisinin-melphalan conjugate, ARS4, exhibited most toxicity to human ovarian cancer cells but had low cytotoxicity to normal cells. ARS4 inhibited the growth and proliferation of ovarian cancer cells and resulted in S-phase arrest, apoptosis, and inhibition of migration; these effects were stronger than those of its parent drugs, DHA and melphalan. Furthermore, ARS4 modulated the expression of proteins involved in cell cycle progression, apoptosis, and the epithelial–mesenchymal transition (EMT). Moreover, in mice, ARS4 inhibited growth and intraperitoneal dissemination and metastasis of ovarian cancer cells without observable toxic effects. Our results provide a basis for development of the compound as a chemotherapeutic agent.

*Research in context:* Artemisinin compounds have recently received attention as anticancer agents because of their clinical safety profiles and broad efficacy. However, their therapeutic potencies are limited by low solubility and poor bioavailability. Here, we report that ARS4, an artemisinin-melphalan conjugate, possesses marked *in-vitro* and *in-vivo* antitumor activity against ovarian cancer, the effects of which are stronger than those for its parent drugs, Dihydroartemisinin and melphalan. In mice, ARS4 inhibits localized growth of ovarian cancer cells and intraperitoneal dissemination and metastasis without appreciable host toxicity. Thus, for patients with ovarian cancer, ARS4 is a promising chemotherapeutic agent.



## 1. Introduction

Ovarian cancer is the sixth leading cause of cancer deaths in women in developed countries and eighth in developing countries (Torre et al., 2015). It is the most lethal gynecologic malignancy, due to the advanced stage of disease at diagnosis, its highly metastatic nature, and lack of effective therapeutic regimens (Jayson et al., 2014; Vaughan et al., 2011). Considerable efforts have been made in evaluating several classes of conventional chemotherapeutic agents, such as paclitaxel and platinum-based agents, for ovarian cancer therapy (Yap et al., 2009). However, the response rates are low, and clinical improvement is marginal, especially for patients with advanced stages of disease, largely due to late diagnoses, persistent dormancy, drug resistance, and cytotoxic side effects (Chen et al., 2013; Janzen et al., 2015; Yap et al., 2009). Therefore, it is necessary to develop new therapeutic agents for ovarian cancer.

We are committed to develop safer and more effective, natural products-based agents for therapy of ovarian cancer (Chen et al., 2009; Chen et al., 2011; Li et al., 2013a). Artemisinin (ARS), a natural sesquiterpene endoperoxide isolated from the plant *Artemisia annua* L, is widely used as an anti-malaria drug (Miller and Su, 2011). ARS and it derivatives also have broad anti-bacterial, anti-inflammatory (Shi et al., 2015), and anti-tumor activities (Firestone and Sundar, 2009). In our previous studies, we found that ARS derivatives, particularly dihydroartemisinin (DHA), exhibit activity against liver cancer cells

* Correspondence to: H. Wang, School of Public Health, Shanghai Jiaotong University School of Medicine, 227 South Chongqing Road, Shanghai, 200025, PR China.
** Correspondence to: H.Liu, Shanghai Institute of Materia Medica, Chinese Academy of Sciences, 555 Zuchongzhi Road, Shanghai, 201203, PR China.
*E-mail addresses:* hliu@mail.shcnc.ac.cn (H. Liu), huiwang@sibs.ac.cn (H. Wang).
[1] These authors contributed equally to this work.

http://dx.doi.org/10.1016/j.ebiom.2016.11.026

and ovarian cancer cells *in vitro* and *in vivo* and sensitize cancer cells to conventional chemotherapeutic agents, such as gemcitabine and carboplatin (Chen et al., 2009; Hou et al., 2008). A reason for developing ARS and its analogs for cancer therapy is the safety profile of this class of compounds, which have been extensively used in the clinic (Lai et al., 2013). We and others have reported that the ARS compounds exert their anticancer effects by inhibiting cell proliferation, inducing cell cycle arrest and apoptosis, inhibiting angiogenesis, reducing cell migration and invasion, and modulating nuclear receptor responsiveness (Chen et al., 2009; Firestone and Sundar, 2009; Hou et al., 2008). However, their therapeutic potencies are limited by their low solubility and poor bioavailability (Steyn et al., 2011). To combat these shortcomings, ARS derivatives have been synthesized and evaluated for their antitumor activities; some demonstrated anti-tumor activity against cultured cancer cells (Blazquez et al., 2013; Buragohain et al., 2015; Crespo-Ortiz and Wei, 2012; Srivastava and Lee, 2015; Zuo et al., 2015). However, only a few of these compounds have been used in practice because of their low efficacy in animal models. Therefore, it is necessary to develop ARS derivatives with better biological activities.

Pharmacophore hybridization, a classical medicinal chemistry strategy, is used widely in drug discovery (Fisher et al., 2014; Romagnoli et al., 2014; Solomon et al., 2010). As described herein, we introduced the pharmacophores of marketed anti-cancer agents into the scaffold of ARS to prepare derivatives by the pharmacophore hybridization strategy. Nine ARS-drug hybrids were designed and synthesized. Compared with the parent drugs, most of the hybrids produced marked cytotoxicity to cancer cells. Of these, the ARS-melphalan conjugate, ARS4, was most toxic to human ovarian cancer cells but had low cytotoxicity to normal cells. ARS4 inhibited the growth and proliferation of ovarian cancer cells A2780 and OVCAR3 and resulted in S-phase arrest, apoptosis, and migration inhibition. These effects were greater than those for its parent drugs, DHA and melphalan. Exposure of cells to ARS4 modulated the expression of proteins involved in cell cycle progression, apoptosis, and the epithelial–mesenchymal transition (EMT). Moreover, in mice, ARS4 inhibited local growth and intraperitoneal dissemination and metastasis of ovarian cancer cells without any appreciable host toxicities. Based on its preclinical efficacy and safety, we conclude that the ARS-melphalan conjugate ARS4 is active as an anti-ovarian cancer agent.

## 2. Materials and Methods

### 2.1. Chemistry

The reagents (chemicals) were purchased from commercial companies and used without further purification unless otherwise stated. Analytical thin-layer chromatography (TLC) was with HSGF 254. All target products were characterized by their NMR, LRMS and HRMS spectra. Chemical shifts are reported in parts per million (ppm, δ) downfield from tetramethylsilane. Proton coupling patterns are described as singlet (s), doublet (d), triplet (t), quartet (q), multipet (m) and broad (br). Low- and high-resolution mass spectra (LRMS and HRMS) were obtained with electric, electrospray, and matrix-assisted laser desorption ionization (EI and ESI) produced by Finnigan MAT-95 and LCQ-DECA spectrometers.

### 2.2. Compounds and Reagents

ARS4 was synthesized from DHA and melphalan at the Shanghai Institute of Materia Medica, Chinese Academy of Sciences (Shanghai, PR China). The chemical structure is shown in Fig. 4A. DHA and carboplatin with purities >98% were purchased from Sigma. Carboplatin (PARAPLATIN) was from NOVAPLUS. The test drugs were dissolved in DMSO and in Cremophor EL:Ethanol:Saline (5:5:90, v/v/v) for *in-vitro* and *in-vivo* study, respectively. Cell Counting Kit-8 (CCK-8) was obtained from Dojindo Laboratories. The ECL Plus system was purchased from Amersham Pharmacia Biotech (Buckinghamshire, UK).

### 2.3. Cell Lines and Cell Culture

Human ovarian epithelial adenocarcinoma cell lines A2780 and OVCAR3 and human ovarian epithelial cell line IOSE144 were obtained from the American Type Culture Collection (ATCC, Manassas, VA, USA). For luciferase stable labeling, A2780 cells were infected by lentivirus expressing firefly luciferase gene obtained from Dr. Dong Xie (Institute for Nutritional Sciences, SIBS, CAS). Cells were cultured in RPMI 1640 medium containing 10% fetal bovine serum, 100 units/ml of penicillin, and 100 μg/ml of streptomycin at 37 °C in a humidified atmosphere with 5% $CO_2$. All cell culture supplies were obtained from Invitrogen-Gibco Co (Grand Island, NY, USA).

### 2.4. Cell Viability

Cell viability was determined with CCK-8 kits, as described previously (Li et al., 2013a; Li et al., 2013b). Briefly, cells were seeded in 96-well plates and were treated either with compounds at serial concentrations or for various times. After 24–72 h of treatment, 10 μl of CCK-8 solution was added to each well, followed by incubation for 3 h. For the determination of IC50 of different compounds, 48 h of incubation was conducted. The absorbance was measured at an optical density of 450 nm using an ApectraMax microplate reader, and the percentage of cell viability was calculated relative to vehicle-treated cells.

### 2.5. Cell-Cycle and Apoptosis Analysis

PI staining was used to detect the effects of ARS-related compounds on cell cycle distribution (Li et al., 2013a; Li et al., 2013b). In brief, after incubation with the compounds, A2780 and OVCAR3 cells were harvested and fixed with 70% ethanol, followed by RNase digestion and staining with PI (50 μg/ml). The cell-cycle distribution was determined with a BD FACS Caliber flow cytometer by quantification of cell DNA contents. Cell apoptosis was determined with Annexin V-fluorescein isothiocyanate (FITC) Apoptosis Detection Kits (BioVision). The floating and trypsinized adherent cells were collected by centrifugation and suspended in binding buffer. Annexin V-FITC and PI were added to the cells before analysis by fluorescence-activated cell sorting (FACS) using a FACSCan flow cytometer (Becton Dickinson). Cell that stained positive for early apoptosis (Annexin V-FITC$^+$/PI$^-$) and for late apoptosis (Annexin V-FITC$^+$/PI$^+$) were combined for the final analysis.

### 2.6. Caspase 3/7 Apoptotic Activity Assay

Caspase-3/7 activity was measured using Caspase-Glo® 3/7 Assay (Promega) assay according to manufacturer's instructions. Routinely, A2780 and OVCAR3 cells were plated 4000/well in 96-well plates, and were treated 5 μM of ARS4 or DHA or melphalan for 24 h. After incubation, 100 μl of Caspase-Glo® 3/7 Reagent was added. Plates were incubated for 1 h prior to reading luminescence in EnSpire Luminescence Microplate Reader (PerkinElmer Inc., USA). No cell sample was used as a background control for luminescence. Caspase 3/7 activity is represented as relative Caspase 3/7 luminescence.

### 2.7. Cell Migration

For cell migration assay, A2780 and OVCAR3 cells were pretreated with indicated concentration of ARS4 for 12 h. Later, Cells were resuspended in serum-free 1640 medium and seeded onto Transwell with an 8 μm microporous membrane (Corning Costar, NY, USA) in 24-well plates. Culture medium with 10% fetal bovine serum was used as a chemoattractant in the lower compartment. Within 12 h, non-invasive cells were carefully removed, and the cells that had migrated to the

lower surface were fixed and stained with crystal violet or eosin. Then, the stained cells were counted. Each experiment was repeated at least three times.

### 2.8. Western Blotting

Immunoblotting was conducted as described previously (Li et al., 2013b). Briefly, A2780 and OVCAR3 cells were separately exposed for 24 h to various concentrations of ARS4 (0, 1, 5, or 10 μM), or to 10 μM of DHA, or to 10 μM of melphalan, and were lysed with RIPA buffer. The total proteins were quantified, separated by SDS-PAGE, and transferred to methanol activated polyvinylidene difluoride (PVDF) membranes. The membranes were blocked with 5% milk and then incubated with primary antibodies against indicated proteins and a secondary antibody. The proteins in the blots were visualized by use of the ECL-Plus system.

### 2.9. Mouse Subcutaneous and Metastasis Models for Ovarian Cancer Chemotherapy.

BALB/c female nude mice (4-week old males) were obtained from the Shanghai Slac laboratory Animal Co. Ltd. The animal use and experimental protocols were approved by the Institutional Animal Care and Use Committee (IACUC) of the Institute for Nutritional Sciences, SIBS, CAS.

For the subcutaneous tumor model, $2 \times 10^6$ A2780 or OVCAR3 cells were injected subcutaneously into the right flanks of 5-week-old female nude mice. Mice bearing tumors about 0.5 cm in diameter were randomized into control and treatment groups ($n = 5$) and were dosed intraperitoneally with vehicle or test compounds for 18 days. Tumor growth and body weights of the mice were monitored every 3 days. Tumor masses were calculated by caliper measurements using the formula "1/2a × b(Asghar et al., 2015)", where "a" is the long diameter and "b" is the short diameter (in mm). For the metastasis model, $2 \times 10^6$ A2780 cells labeled with luciferase were injected intraperitoneally into nude mice, a model for which the gross pathology and pattern of dissemination of tumor nodules resemble human metastatic ovarian cancer (Naora and Montell, 2005; Sale and Orsulic, 2006). The establishment and growth of tumors were monitored by bioluminescent imaging with the Xenogen imaging system (IVIS) as described previously (Li et al., 2015). Mice bearing tumors were grouped into the treatment and control groups (8/group) according to the level of bioluminescence. During the course of treatment, mice were imaged at indicated times.

### 2.10. H&E Staining and Pathological Analysis

The tissues were fixed and embedded in paraffin and sectioned into 4-μm slices. Tissue sections were then deparaffinized in xylenes, rehydrated, and stained with hematoxylin and eosin (H&E). All the slides were analyzed and viewed under Vectra automated quantitative pathology imaging system (PerkinElmer Inc., USA).

### 2.11. Statistical Analysis

Values are presented as means ± SEM from at least three independent experiments. For single group analysis, unpaired two-sided *t*-test or one-way ANOVA was used to test the significance of differences, followed by Tukey's multiple comparisons; for grouped analysis, two-way ANOVA was used, followed by Bonferroni post-tests. $P < 0.05$ was considered significant.

## 3. Results

### 3.1. Chemistry

We introduced the pharmacophores of five clinical anti-cancer agents, chlorambucil (**2**), melphalan (**3**), flutamide (**4**), aminoglutethimide (**5**) and doxifluridin (**6**) into the scaffold of DHA (**1**) (Fig. S1a), thus acquiring derivatives (**7–15**) by the pharmacophore hybridization strategy (Fig. S1 and Fig. S2). The pharmacophores of the chlorambucil (**2**) and melphalan (**3**) were introduced into the scaffold of DHA to give the derivatives **7, 9,** and **10** *via* a simple condensation reaction (**Fig. S1b**). 10β-(3-Tosyl-propyl)-deoxoartemisinin (**17**) was prepared by treatment of 10β-(3-propanol)-deoxoartemisinin with tosyl chloride (**16**) and was easily obtained according to a reported method (Chadwick et al., 2009) followed by treating with piperazine to give the key intermediate **18**. The target compound **8** was obtained from **18** in a similar manner as depicted for the preparation of product **7** (Fig. S1b). Similarly, hybrids **11–15** were synthesized from artesunate derivatives with the moieties of anti-cancer drugs, melphalan, flutamide, aminoglutethimide, and doxifluridin by a condensation reaction (Fig. S2).

### 3.2. Structure-Activity Relationship of ARS-Chemotherapeutic Agent Conjugates

Screening was conducted to examine the effects of ARS-drug hybrids (**7–15**) on the viability of various tumor cells and normal cells. Human liver cancer cells (HepG2 and Hep3B), human ovarian cancer cells (A2780 and OVCAR3), human breast cancer cells (MCF7, MDA-MB-231), human prostate cancer cells (PC-3 and DU145), and their paired normal cells (7702, IOSE144 and MCF10A) were exposed to various concentrations of the drug hybrids **7–15** and to the parent drugs, DHA, chlorambucil, melphalan, flutamide, aminoglutethimide, and doxifluridin. The results, expressed as $IC_{50}$ values (μM) are summarized in Supplementary Table 1. Compared with the parent drugs, most of the ARS-drug hybrids caused growth inhibition of human liver cancer and ovarian cancer cells with $IC_{50}$ values $<10$ μM. The hybrids and their parent drugs, with $IC_{50}$ values $>50$ μM, had less cytotoxicity to human breast and prostate cancer cells.

### 3.3. ARS4 Exhibits Potent Cytotoxicity to Human Ovarian Cancer Cells

On the basis of screening for tumoricidal activity, the ARS-melphalan conjugate analog **9** (ARS4, Fig. 1a) was most effective. ARS4 showed an extensive tumor-killing effect on human ovarian cancer cells (IC50 values: A2780, 0.86 μM; OVCAR3: 0.83 μM; Fig. 1b–d). Of note, the tumoricidal activity of ARS4 was greater than that of its parent compounds, DHA (IC50 value: A2780, 4.75 μM; OVCAR3: 5.65 μM; Fig. 1b–d) and melphalan (IC50 value: A2780, 23.18 μM; OVCAR3: 11.61 μM; Fig. 1b–d). Normal ovarian epithelial cells (IOSE144), incubated with ARS4 for 48 h, exhibited less cytotoxicity, with an IC50 of 43.64 μM, indicating that ARS4 selectively killed cancer cells (Fig. 1b and Fig. S3). ARS4 inhibited cancer cell growth in a concentration-dependent manner, showing 59.2% and 67.1% inhibition at 1 μM for A2780 and OVCAR3 cells, respectively. By comparison, normal cells IOSE144 were less sensitive, with 6% inhibition at the same concentration (Fig. S3). Moreover, a time-course assay demonstrated that ARS4 inhibited the proliferation of A2780 and OVCAR3 cells in a concentration-dependent manner (Fig. 1f).

These data indicate that ARS4 selectively inhibits ovarian cancer cell growth and proliferation and that this conjugate exhibits more potency than its parent drugs, DHA and melphalan.

### 3.4. ARS4 Induces Apoptosis in Human Ovarian Cancer Cells and Changes in the Expression of Apoptosis Related Proteins

Our previous reports have demonstrated that ARS and its derivative DHA have anticancer effects against human ovarian cancer cells and hepatoma cells *via* inducing cell apoptosis and G1-phase arrest (Chen et al., 2009; Hou et al., 2008). To examine the mechanism responsible for the greater anticancer effect in comparison with DHA and melphalan, we determined if ARS4 had an enhanced effect on apoptosis and

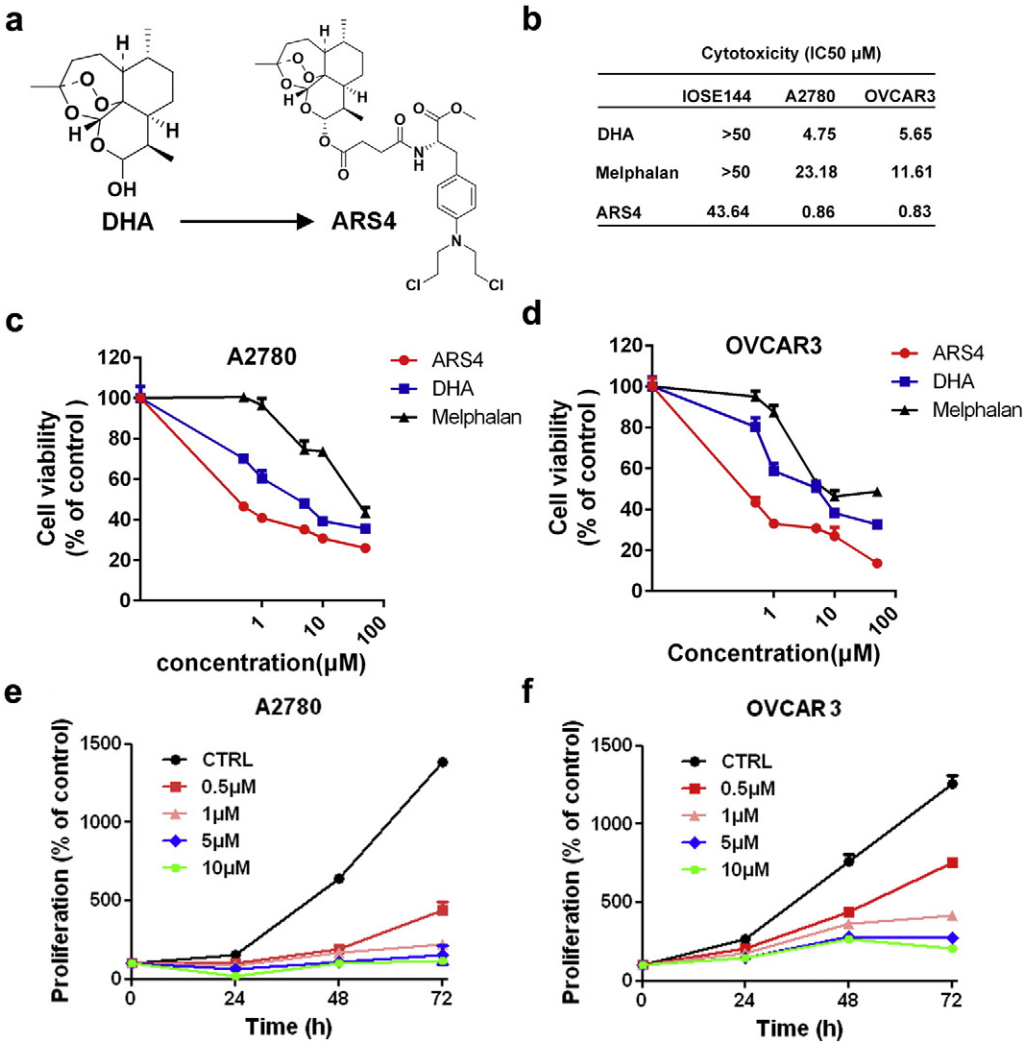


**Fig. 1.** Cytotoxicity of ARS4 against human ovarian normal and cancer cells. **(a)** The design strategy and chemical structure of ARS4. **(b)** $IC_{50}$ values of ARS4 and its parent compounds, DHA and melphalan, for human ovarian cancer cells, A2780 and OVCAR3, and human ovarian epithelial cells, IOSE144. Cytotoxicity was assessed by CCK8 assays after 48 h of incubation with the indicated compounds. Viability of A2780 **(c)** and OVCAR3 cells **(d)** after exposure to ARS4 and its parent drugs DHA and melphalan at various concentrations for 48 h. Inhibition of proliferation of A2780 **(e)** and OVCAR3 **(f)** cells after exposure to ARS4 for 0, 24, 48, or 72 h.

cell cycle arrest. ARS4 induced apoptosis in A2780 and OVCAR3 cells in a dose-dependent manner (Fig. 2a–b), an effect greater than that of DHA at the same concentration (Fig. 2d). By comparison, normal cells IOSE144 were less apoptotic when exposed to ARS4 at the same concentration, indicating the selective activity of ARS4 against cancer cells (Fig. 2c). Assay of caspase 3/7 apoptotic activity showed that the level of active caspase 3/7 in the A2780 and OVCAR3 cells treated with ARS4 was significantly higher than that for DHA and melphalan at the same concentration (Fig. 2e).

Activated by caspase 9, caspase 3, is an executioner caspase cleaved a broad spectrum of target proteins, such as PARP, leading to a cell death cascade (Bressenot et al., 2009). To define how the apoptotic pathway was activated by ARS4, the activation of caspase 3 and PARP in cells treated with ARS4 or their parent compounds was evaluated. Exposure of OVCAR3 cells to ARS4 resulted in a dose-dependent increase in the cleavage of caspase 3 and PARP (Fig. 2f). With the same treatment, there was also elevated cleaved caspase 3 in A2780 cells, while no obvious PARP cleavage was observed (Fig. 2f). In contrast, DHA and melphalan had less effect on the cleavage of caspase 3 and PARP (Fig. 2f). ARS4 downregulated Bcl-2, a protein involved in regulation of apoptosis (Fig. 2f). This indicates that the mitochondrial apoptotic pathway is activated preferentially by ARS4. The PI3K/AKT and MAPK/ERK pathways are mediators of cell growth and survival (Asati et al., 2016; Ewald et al., 2014; Saini et al., 2013). For both types of cells, ARS4 treatment resulted in a dose-dependent inactivation of the PI3K/AKT and MAPK/ERK pathways as reflected by reduced total AKT and dephosphorylation of AKT, mTOR, and ERK (Fig. 2f).

### *3.5. ARS4 Induces S-Phase Arrest of the Cell Cycle and Down-Regulates Cyclins and Cdks*

To determine if ARS4 inhibited cell-cycle progression, A2780 and OVCAR3 cells were exposed to various concentrations of ARS4 for 24 h, and the distribution of cells in the cell cycle was determined by propidium iodide (PI) staining and flow cytometric analysis. For both types of cancer cells, treatment for 24 h with ARS4 induced a significant accumulation of cells in S phase in a concentration-dependent manner and a concomitant decrease in the number of cells inG1 and G2/M phases (Fig. 3a and b). Interestingly, ARS4 had less effect on the cell cycle progression in normal cells IOSE144 and S-phase arrest was observed when incubated with higher concentration (10 μM) of ARS4

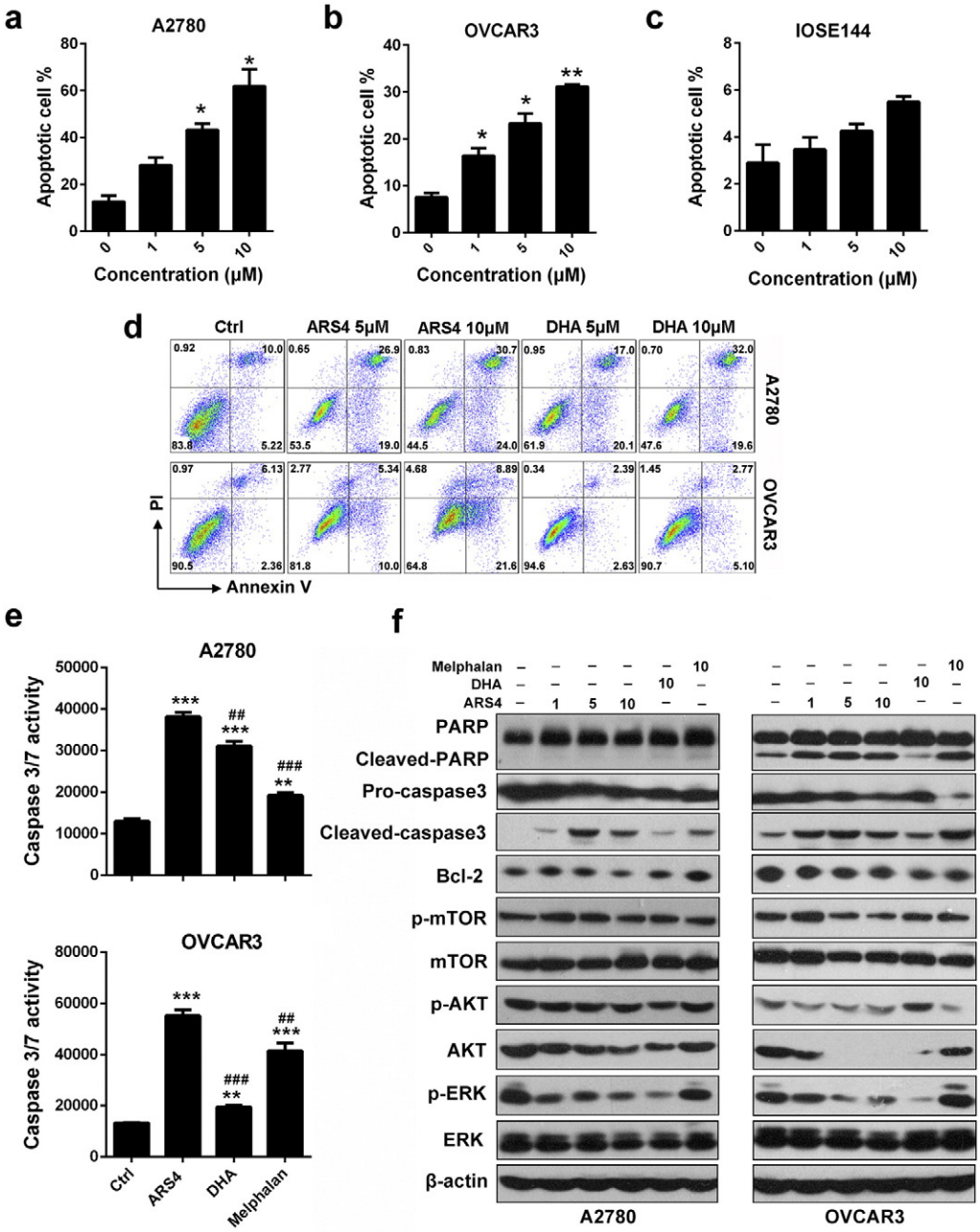


**Fig. 2.** ARS4 selectively induces apoptosis on ovarian cancer cells *in vitro* **(a–c)** Effects of ARS4 on cell apoptosis. Human ovarian cancer cells A2780 **(a)** and OVCAR3 **(b)** and normal cell IOSE144 cells **(c)** were exposed to various concentrations (0, 1, 5, and 10 μM) of ARS4 for 24 h, followed by measurement of apoptosis by the Annexin V assay. **(d)** Representative flow cytometry data showing the proportion of apoptotic A2780 and OVCAR3 cells after incubation with the same concentration of ARS4 or DHA. **(e)** Activation of caspase 3/7 in ovarian cancer cells after incubation for 24 h with 5 μM of ARS4, DHA or melphalan. **(f)** The expression of proteins related to apoptosis was determined by Western blotting assays. The data shown are representative of values from 3 independent experiments with similar results (means ± SEM; $^{*}P < 0.05$, $^{**}P < 0.01$, $^{***}P < 0.001$ with respect to the control; $^{\#}P < 0.05$, $^{\#\#}P < 0.01$, $^{\#\#\#}P < 0.001$ with respect to ARS4 treatment).

(Fig. 3c). The cell-cycle progression of cells treated with ARS4, DHA, or melphalan was compared. DHA induced a modest arrest in the G0/G1 phase; melphalan arrested cells in the S phase (Fig. 3d).

Since Cdks, Cdk inhibitors, and cyclins are involved in regulation of cell cycle progression (Asghar et al., 2015; Delaval and Birnbaum, 2007), the expression of these proteins in A2780 and OVCAR3 cells treated with ARS4, DHA or melphalan were examined. In both types of cells, treatment with ARS4 resulted in a marked reduction in the expression of cyclin D and CDK4 and less change in cyclin A. In contrast, DHA downregulated cyclin A, but had little effect to the expressions of cyclin D and CDK4 (Fig. 3e). These protein patterns correlated the cell-cycle distributions resulting from treatment with ASR4 or DHA. The expressions of cyclin E and E2F1 were downregulated in both types of cells treated with ARS4 or DHA (Fig. 3e). Analysis of the expression of p53, MDM2, p21, and p27 indicated that ARS4 decreased the expression of MDM2 and p27, but increased the expression of p21; DHA had a similar effect (Fig. 3e). In cells treated with melphalan, there were no apparent changes in CDKs and cyclins, except for the downregulation of p27 and upregulation of p21 (Fig. 3e), indicating the different anticancer mechanisms for ARS4, DHA, and melphalan. These observations suggest that the downregulation of CDKs and cyclins and upregulation of the CDK inhibitor p21 are involved in the S-phase arrest in cells treated with ARS4. The molecular mechanism is different from those of its parent compounds.

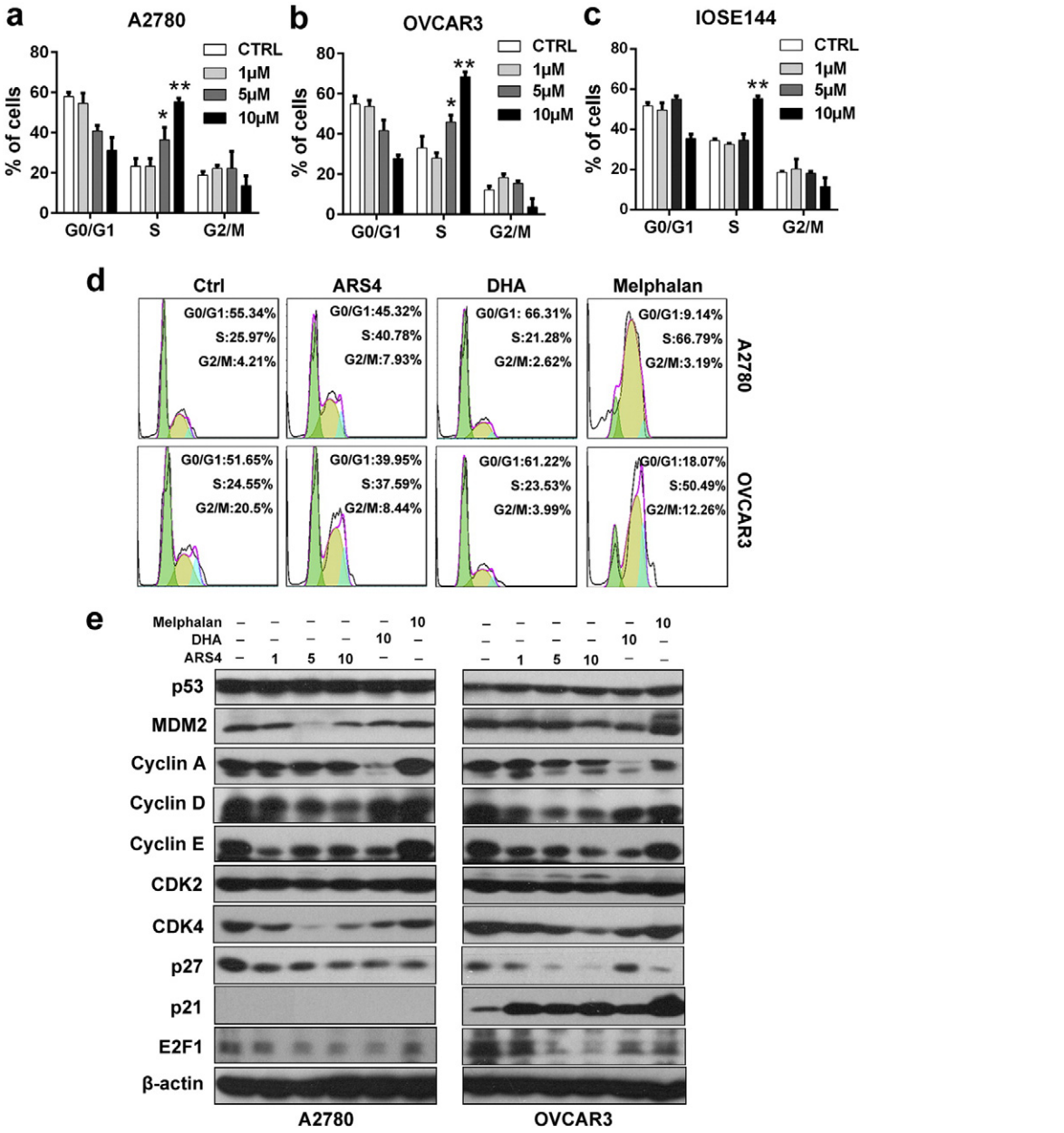


**Fig. 3.** ARS4causes dose-dependent S-phase cell cycle arrest of ovarian cancer cells *in vitro* **(a–c)** Effects of ARS4 on cell cycle progression. A2780 **(a)**, OVCAR3 **(b)**, and IOSE144 **(c)** cells were exposed to various concentrations (0, 1, 5, and 10 μM) of ARS4 for 24 h, followed by determination of cell cycle distribution using flow cytometry (means ± SEM; * $P < 0.05$, ** $P < 0.01$). **(d)** Representative flow cytometry data showing the percentage distributions for specific phases of cells treated with the same concentration (5 μM) of ARS4, DHA or melphalan. **(e)** The expression of proteins related to cell cycle was determined by Western blotting assay.

### *3.6. ARS4 Inhibits Cell Migration of Cultured Human Ovarian Cancer Cells and Reverses EMT Polarity.*

Metastasis, which leads to morbidity and eventual mortality, remains a challenge in the clinical man agement of ovarian cancer (Naora and Montell, 2005). Thus, the effect of ARS4 on ovarian cancer cell migration after 12 h of exposure was evaluated (Fig. 4a). ARS4 inhibited A2780 and OVCAR3 cell migration to a greater extent than DHA (Fig. 4a). To rule out the possibility that the inhibitory effect of ARS4 and DHA on migration resulted from cytotoxicity, the growth of cells after 12 h of exposure to the compounds was measured by the CCK8 assay. There was no apparent inhibition of growth of ovarian cancer cells (data not shown).

Changes in cell phenotype from epithelial to mesenchymal, defined as EMT, are involved in the pathogenesis of ovarian cancer in terms of increase of cell motility and invasiveness and acquisition of resistance to apoptosis (Gao and Mittal, 2012; Gao et al., 2012; Thiery et al., 2009). A2780 and OVCAR3 cells treated with ARS4 exhibited a repressed EMT phenotype, that is, up-regulation of the epithelial marker E-cadherin and downregulation of the mesenchymal marker Vimentin and EMT-related transcription factors Snail and Slug (Fig. 4b); this effect of ARS4 was stronger than that in cells exposed to DHA (Fig. 4b). In contrast, melphalan had no obvious effect on the expression of EMT-related proteins (Fig. 4b). This result is consistent with inhibition of migration and induction of cell apoptosis by ARS4.

These results establish that ARS4 exerts its anticancer activity through arrest of cell cycle progression in the S-phase, by induction of apoptosis through the mitochondrial pathway, by suppression of cell motility, and by repressing the EMT transition.

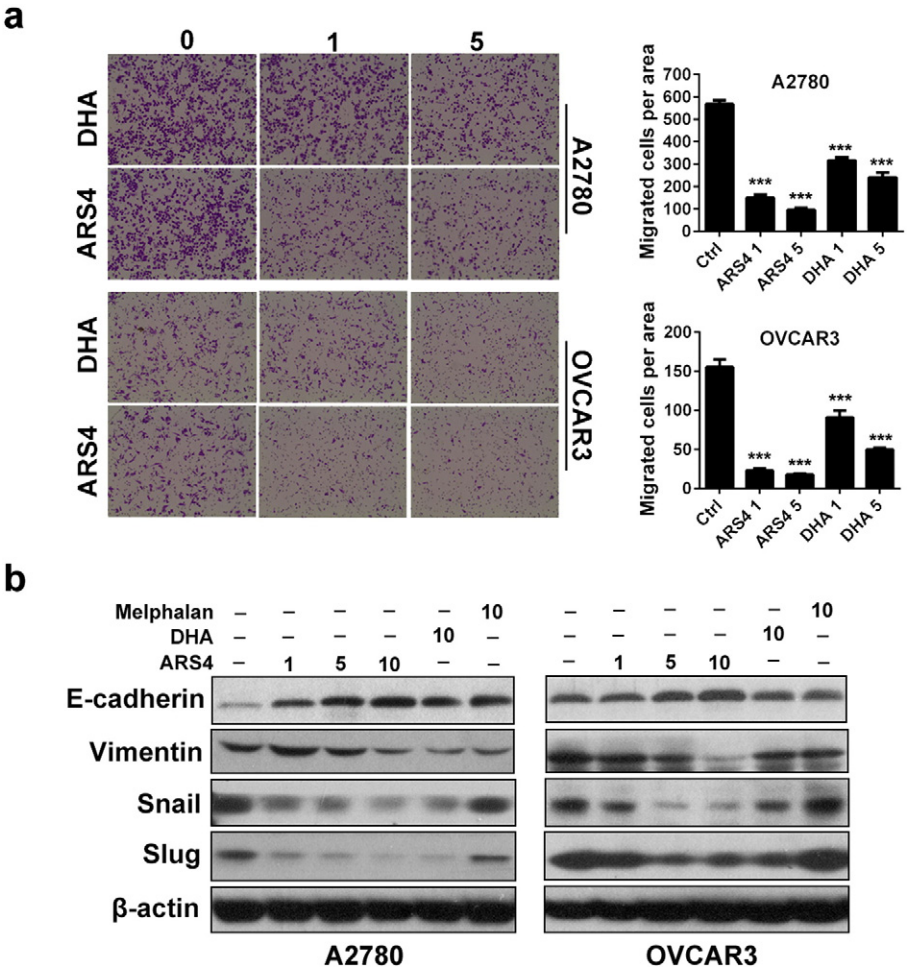


**Fig. 4.** ARS4 inhibits ovarian cancer cell migration and the EMT process. **(a)** Results of cell migration assays using A2780 and OVCAR3 cells treated with ARS4 or DHA for 12 h (means ± SEM, $n = 3$, *** $p < 0.001$ *versus* the control treatment). **(b)** Expression of the epithelial protein, E-cadherin, the mesenchymal proteins, Vimentin, and E-cadherin; and the transcription suppressors, Snail and Slug, in A2780 and OVCAR3 cells, as detected by Western blotting after 24 h exposure to the indicated compounds. The numbers showed μM concentrations.

### *3.7. ARS4 Inhibits Growth of Subcutaneous Ovarian Cancer Cells and Intraperitoneal Dissemination and Metastasis.*

The effects of ARS4 on growth of xenografts of human ovarian tumors and on metastasis of these cells were evaluated. BALB/c nude mice bearing subcutaneous xenografts of A2780 and OVCAR3 cells were treated with ARS4 at doses of 5 mg/kg, 10 mg/kg, or 25 mg/kg for 18 days. Therapeutic effects were evaluated by assessing tumor growth. ARS4, at doses of 10 and 25 mg/kg, resulted in 58% and 74% inhibition of growth of A2780 xenografts (Fig. 5a) and 66% and 83% in the OVCAR3 xenografts, respectively (Fig. 5b). Moreover, based on body weights, ARS4 caused no appreciable toxic effect (Fig. 5a–b).

The effects of ARS4 on ovarian cancer cell dissemination and metastasis were investigated by use of immunodeficient mice that were intraperitoneally injected with A2780 cells labeled with firefly luciferase. The mice bearing A2780 tumors were treated with vehicle or with ARS4 at a dose of 25 mg/kg for 18 days. Tumor growth and progression were monitored by bioluminescent imaging with the Xenogen IVIS imaging system. Mice treated with the vehicle developed tumors in organs throughout the peritoneal cavity, and the bioluminescence signal increased progressively with time (Fig. 5c–d). By comparison, in mice that received 25 mg/kg of ARS4, tumor progression and bioluminescence signals were inhibited (Fig. 5c–d). Western blotting with tumor tissue samples also showed that treatment with ARS4 led to the repression of the EMT phenotype, *i.e.*, the upregulation of E-cadherin and downregulation of Vimentin, Snail and Slug (Fig. 5e).

### *3.8. ARS4 Exhibits More Potent Therapeutic Efficacy and Preclinical Safety than its Parent Drugs*

To compare the potency and safety of ARS4 and its parent drugs, an efficacy study was performed with mice bearing A2780 and OVCAR3 tumor xenografts. To evaluate host toxicity, histological examinations on major organs (liver, spleen, kidneys and lung) were conducted. ARS4, DHA, and melphalan (25 mg/kg) were administered daily for 14 days. Carboplatin (25 mg/kg), a clinically used chemotherapeutic agent for ovarian cancer, was included as a comparative drug (Fig. 6a–b). ARS4 inhibited the growth of A2780 and OVCAR3 xenograft tumors by 68% and 76%, and DHA inhibited by 50% and 51%, respectively; Carboplatin had a moderate effect with 25% and 40% inhibitions, respectively (Fig. 6a–b and Fig. S4a–b). Of note, ARS4 exhibited much better solubility than DHA in the bioassay solvent system of our *in vivo* therapeutic experiments (Fig. S4c). There were no significant changes in the average body weights of the mice treated with ARS4, DHA or Carboplatin, suggesting that the treatment did not result in host toxicity (Fig. 6a–b). In comparison, severe toxicity was evident in mice treated with 25 mg/kg of melphalan, as indicated by a severe loss of body weight, this experiment was terminated for animal welfare at day 8 (Fig. 6a–b).

At the end of the experiments, various organs (liver, kidneys, spleen and lung) were removed from mice; these were weighted and dissected for histological examinations. There were no significant differences in tissue weights between the vehicle and ARS4 treatment groups,

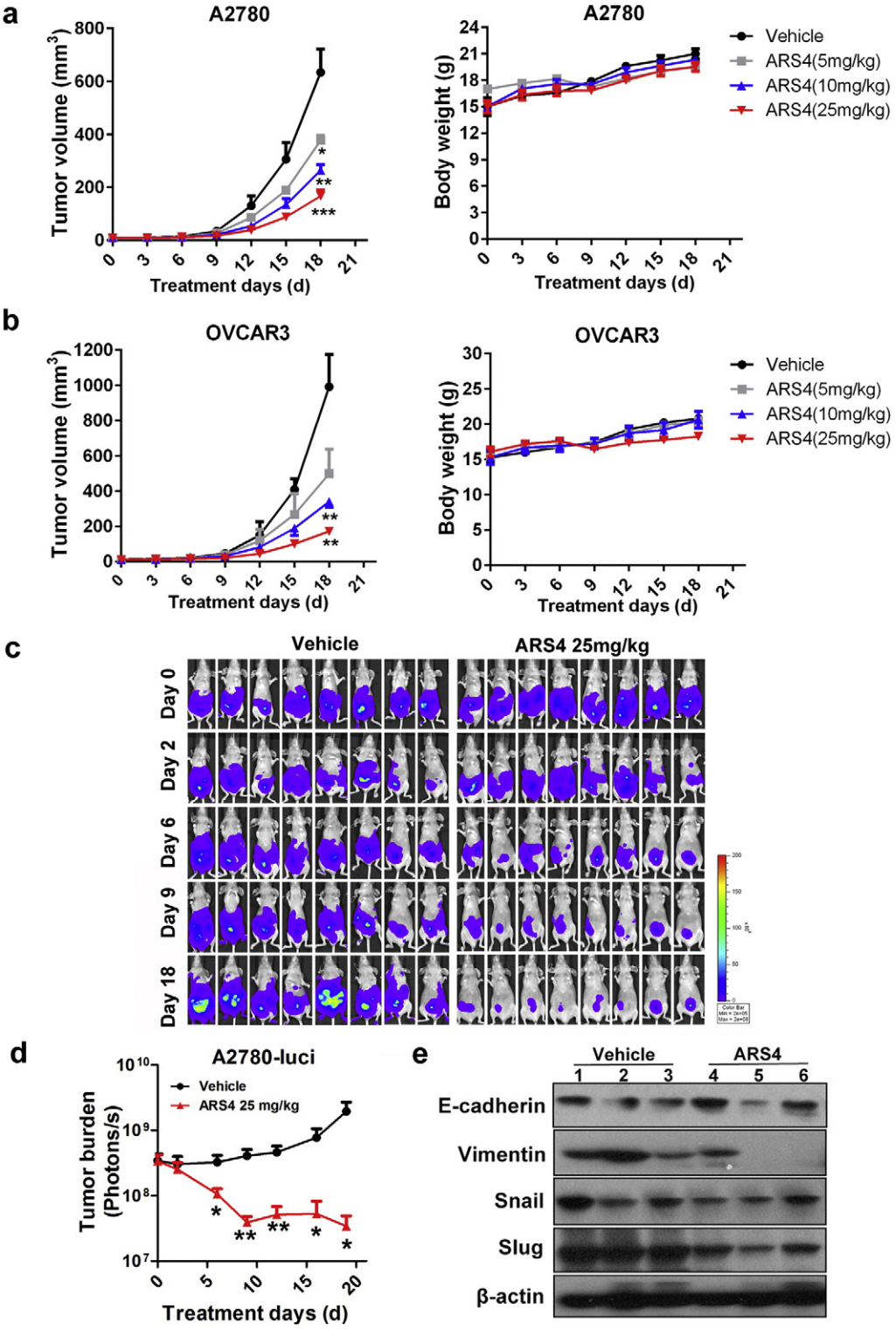


**Fig. 5.** ARS4 inhibits tumor growth and metastasis in mice bearing xenografted ovarian tumor cells. **(a–b)** Human ovarian cancer cells A2780 **(a)** and OVCAR3 **(b)** were separately transplanted into the right sides of nude mice, which were treated intraperitoneally daily with ARS4 at doses of 5 mg/kg, 10 mg/kg, or 25 mg/kg for 18 days. Tumor growth was measured every 3 days. Animals were also monitored for changes of body weight as a marker for toxicity. Data are presented as means ± SEM ($n = 5$, * $p < 0.05$, ** $p < 0.01$, *** $p < 0.001$ *versus* the control treatment). **(c)** Representative bioluminescence images of mice treated with ARS4 (25 mg/kg) or the vehicle at the indicated times after intraperitoneal injection of luciferase-labeled A2780 cells. **(d)** Quantification of the bioluminescence by live imaging showed greater tumor growth in the vehicle group relative to the treated group (means ± SEM; * $p < 0.05$, ** $p < 0.01$; $n = 8$). **(e)** The results of a Western blot analyse showing the expression of EMT-related protein in tumors treated with ARS4 (25 mg/kg) or the vehicle. The numbers indicate individual tumors.

indicating that ARS4 treatment was safe at therapeutic doses (Fig. 6c–f). Similar effects were found for mice treated with DHA or Carboplatin, except for weight gain of spleens in the DHA group and loss in the Carboplatin group (Fig. 6c–f). Severe decreases in organ weight (liver, kidneys and spleen) were evident in melphalan treated mice (Fig. 6c–f). In addition, in the tissues examined (liver, kidneys, spleen, and lung), there were no obvious differences in the histological findings between the control and treatment groups (Fig. 6g and Fig. S4d). However,

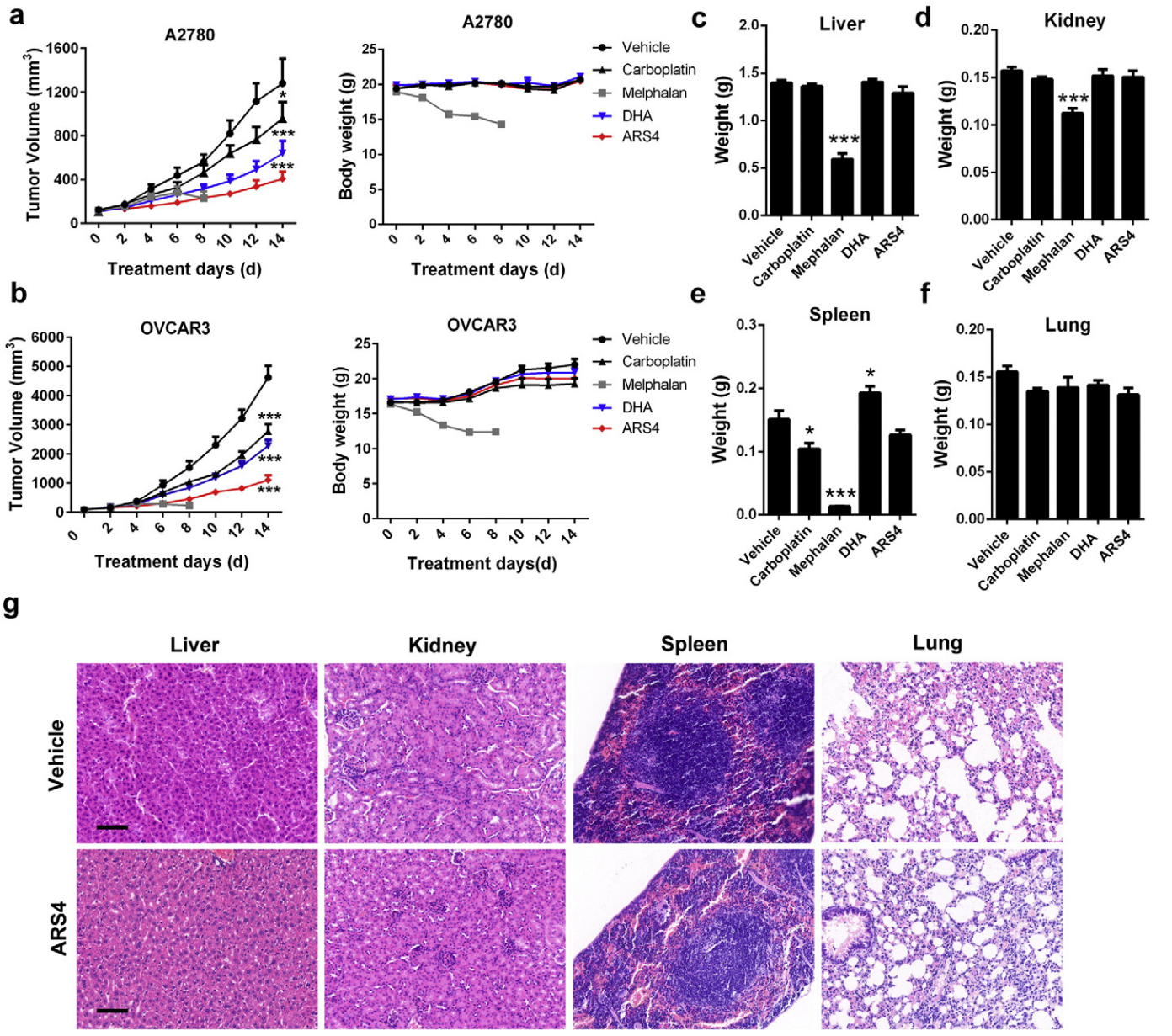


**Fig. 6.** ARS4 exhibits more potent therapeutic efficacy and a more favorable safety profiles than its parent drugs **(a–b)** Mice bearing A2780 **(a)** or OVCAR3 tumors **(b)** were treated intraperitoneally daily with ARS4, DHA, melphalan or carboplatin at doses of 25 mg/kg for 14 days. Tumor growth and body weight were measured every 2 days. Severe toxicity was observed evident in mice treated with melphalan, as indicated by a significant severe loss of body weight loss; and this experiment was terminated for animal welfare at day 8. **(c)** At the end of experiments, mice were sacrificed and various organs (liver, kidneys, spleen and lung) were removed from mice and weighted (means ± SEM; * $p < 0.05$, ** $p < 0.01$, *** $p < 0.001$; $n = 6$). **(d)** To evaluate host toxicity, histological examinations of major organs were conducted. H&E staining of these tissues was shown (Scale bars, 200 μm).

substantial necrosis of liver and spleen parenchymal cells was found in mice dosed with melphalan, suggesting the presence of host toxicity (Fig. S4d).

These results show that, for xenografts of ovarian cancer, ARS4 has impressive therapeutic efficacy without an appreciable toxic effect.

## 4. Discussion

Although traditional chemotherapy remains the mainstay for treatment of human ovarian cancer, the response rates for most chemotherapeutic agents are low, and clinical improvement is marginal (Vaughan et al., 2011; Yap et al., 2009). In addition, severe toxicities and drug resistance often occur, reducing the quality of life for patients and hindering the effective application of these agents (Chen et al., 2013; Janzen et al., 2015; Jayson et al., 2014; Yap et al., 2009).

Because of their structural diversity and promising therapeutic applications, natural products and their derivatives have caught the attention of pharmacologists and chemists. ARS and its derivatives are demonstrated to have excellent anticancer effects both *in vitro* and *in vivo* (Chen et al., 2009; Firestone and Sundar, 2009; Hou et al., 2008). However, their therapeutic potencies are limited by low solubility and poor bioavailability (Steyn et al., 2011), it is necessary to prepare ARS derivatives with better biological activities. Recently, increasing attention has been focused on designation and synthesis of new ARS derivatives and on evaluating their antitumor activity (Buragohain et al., 2015; Crespo-Ortiz and Wei, 2012; Njuguna et al., 2012). Several studies demonstrate that ARS related compounds were effective to many types of cancer cell lines and even multiple drug- and radiation-resistant ones due to their multiple mechanisms (Sadava et al., 2002; Xie et al., 2011). As the applications of pharmacophore hybridization strategy to synthesize ARS derivatives are emerging (Sadava et al., 2002; Yang et al.,

2009), it is reasonable to combine ARS pharmacophoric scaffold with clinically used chemotherapeutic agents to form a single molecular framework, which would enable us to find more potent antitumor agents.

Through a pharmacophore hybridization strategy, we designed and synthesized nine ARS-drug conjugates with different bulky group at position C10 of DHA, in which the marketed drugs chlorambucil, melphalan, flutamide, aminoglutethimide, and doxifluridine were respectively bonded to ARS nucleus through different linkages. Biological evaluations demonstrated that these hybrids had more cytotoxicity to cancer cells than the parent drugs. Among these conjugates, the artemisinin-melphalan conjugate, ARS4, exhibited the highest toxicity to ovarian cancer cells and had low cytotoxicity to normal cells. ARS4 inhibited the growth and proliferation of A2780 and OVCAR3 ovarian cancer cells and resulted in S-phase arrest, apoptosis, and inhibition of migration; these effects were stronger than those for its parent drugs, DHA and melphalan. Furthermore, exposure of cells to ARS4 modulated the expression of proteins involved in cell cycle progression, apoptosis, and the EMT, leading to increases in the levels of p21, E-cadherin, cleaved-PARP, and cleaved caspase 3 and to decreases of Mdm2, cyclin D, cyclin E, CDK4, E2F1, Bcl-2, Vimentin, Snail and Slug. PI3K/AKT and MAPK pathways play essential role in cell growth, cell proliferation, apoptosis and metastasis (Cotrim et al., 2013; Ingeson-Carlsson and Nilsson, 2014; Schultze et al., 2012; Thompson et al., 2015), which are also the central regulators EMT phenotype (Elsum et al., 2013; Larue and Bellacosa, 2005; Mulholland et al., 2012). We further demonstrated that ARS4 inactivated PI3K/AKT and MAPK pathway with respect to down-regulation of phosphorylated AKT, mTOR, and ERK.

Melphalan is a clinical-used alkylating antitumor agent and is often the drug of choice in the treatment of ovarian, melanoma, and breast cancer. Melphalan, shows a diversity of toxic side effects especially when used at a high dose (Casanova et al., 2012). Currently, we proved that ARS4, an artemisinin-melphalan conjugate, markedly inhibited local growth and intraperitoneal dissemination and metastasis of xenografts of ovarian cancer cells with no observable toxic effects, and showed improved water-solubility and increased potency and safety related to DHA and melphalan.

In summary, series of hybrid ARS derivatives conjugated with clinically used chemotherapeutic agents were designed and synthesized based on the hybrid strategy. On the basis of their efficacy in cell cultures and in mice, these ARS-drug hybrids, particularly ARS4, are promising as lead compounds for development of chemotherapeutic agents for the treatment of ovarian cancer.

## Conflict-of-Interest Disclosure

The authors declare no actual or potential competing financial interests.

## Author Contributions

X.L., Y.Z., H.L. and H.W. designed the experiments. X.L., Y.Z., H.L. and H.W. analyzed the data and wrote the manuscript. H.L. and H.W. supervised the project. X.L., Y.L., T.C., Q.B., and J.L. performed the *in vitro* and *in vivo* potency and safety evaluation. Y.Z., X.Z. K.C. carried out the drug design and chemical synthesis. All authors reviewed and approved the manuscript.

## Acknowledgements

We thank Dr. Donald L. Hill for assistance in preparation of this manuscript. This study was supported by grants from the National Nature Science Foundation (81630086, 91529305, 81302809, 81672763 and 81502122), the Strategic Priority Research Program (XDA12020319) of the Chinese Academy of Sciences, the Science and Technology Commission of Shanghai Municipality (14391901800), and the Food Safety Research Center and Key Laboratory of Food Safety of INS, SIBS, CAS.

## Appendix A. Supplementary data

Supplementary data to this article can be found online at http://dx.doi.org/10.1016/j.ebiom.2016.11.026.

## References

Asati, V., Mahapatra, D.K., Bharti, S.K., 2016. PI3K/Akt/mTOR and Ras/Raf/MEK/ERK signaling pathways inhibitors as anticancer agents: structural and pharmacological perspectives. J Med Chem.]–>Eur. J. Med. Chem. 109, 314–341.

Asghar, U., Witkiewicz, A.K., Turner, N.C., Knudsen, E.S., 2015. The history and future of targeting cyclin-dependent kinases in cancer therapy. Nat. Rev. Drug Discov. 14, 130–146.

Blazquez, A.G., Fernandez-Dolon, M., Sanchez-Vicente, L., Maestre, A.D., Gomez-San Miguel, A.B., Alvarez, M., Serrano, M.A., Jansen, H., Efferth, T., Marin, J.J., et al., 2013. Novel artemisinin derivatives with potential usefulness against liver/colon cancer and viral hepatitis. Bioorg. Med. Chem. 21, 4432–4441.

Bressenot, A., Marchal, S., Bezdetnaya, L., Garrier, J., Guillemin, F., Plenat, F., 2009. Assessment of apoptosis by immunohistochemistry to active caspase-3, active caspase-7, or cleaved PARP in monolayer cells and spheroid and subcutaneous xenografts of human carcinoma. J. Histochem. Cytochem. 57, 289–300.

Buragohain, P., Surineni, N., Barua, N.C., Bhuyan, P.D., Boruah, P., Borah, J.C., Laisharm, S., Moirangthem, D.S., 2015. Synthesis of a novel series of fluoroarene derivatives of artemisinin as potent antifungal and anticancer agent. ACS Med. Chem. Lett. 25, 3338–3341.

Casanova, F., Quarti, J., da Costa, D.C., Ramos, C.A., da Silva, J.L., Fialho, E., 2012. Resveratrol chemosensitizes breast cancer cells to melphalan by cell cycle arrest. J. Cell. Biochem. 113, 2586–2596.

Chadwick, J., Mercer, A.E., Park, B.K., Cosstick, R., O'Neill, P.M., 2009. Synthesis and biological evaluation of extraordinarily potent C-10 carba artemisinin dimers against *P. falciparum* malaria parasites and HL-60 cancer cells. Bioorg. Med. Chem. 17, 1325–1338.

Chen, T., Li, M., Zhang, R., Wang, H., 2009. Dihydroartemisinin induces apoptosis and sensitizes human ovarian cancer cells to carboplatin therapy. J. Cell. Mol. Med. 13, 1358–1370.

Chen, T., Xu, Y., Guo, H., Liu, Y., Hu, P., Yang, X., Li, X., Ge, S., Velu, S.E., Nadkarni, D.H., et al., 2011. Experimental therapy of ovarian cancer with synthetic makaluvamine analog: in vitro and in vivo anticancer activity and molecular mechanisms of action. PLoS One 6, e20729.

Chen, X., Zhang, J., Zhang, Z., Li, H., Cheng, W., Liu, J., 2013. Cancer stem cells, epithelial-mesenchymal transition, and drug resistance in high-grade ovarian serous carcinoma. Hum. Pathol. 44, 2373–2384.

Cotrim, C.Z., Fabris, V., Doria, M.L., Lindberg, K., Gustafsson, J.A., Amado, F., Lanari, C., Helguero, L.A., 2013. Estrogen receptor beta growth-inhibitory effects are repressed through activation of MAPK and PI3K signalling in mammary epithelial and breast cancer cells. Oncogene 32, 2390–2402.

Crespo-Ortiz, M.P., Wei, M.Q., 2012. Antitumor activity of artemisinin and its derivatives: from a well-known antimalarial agent to a potential anticancer drug. J. Biomed. Biotechnol. 247597.

Delaval, B., Birnbaum, D., 2007. A cell cycle hypothesis of cooperative oncogenesis (review). J Oncol.]–>Int. J. Oncol. 30, 1051–1058.

Elsum, I.A., Martin, C., Humbert, P.O., 2013. Scribble regulates an EMT polarity pathway through modulation of MAPK-ERK signaling to mediate junction formation. J. Cell Sci. 126, 3990–3999.

Ewald, F., Norz, D., Grottke, A., Hofmann, B.T., Nashan, B., Jucker, M., 2014. Dual inhibition of PI3K-AKT-mTOR- and RAF-MEK-ERK-signaling is synergistic in cholangiocarcinoma and reverses acquired resistance to MEK-inhibitors. Investig. New Drugs 32, 1144–1154.

Firestone, G.L., Sundar, S.N., 2009. Anticancer activities of artemisinin and its bioactive derivatives. Expert Rev. Mol. Med. 11, e32.

Fisher, G.M., Tanpure, R.P., Douchez, A., Andrews, K.T., Poulsen, S.A., 2014. Synthesis and evaluation of antimalarial properties of novel 4-aminoquinoline hybrid compounds. Chem. Biol. Drug Des. 84, 462–472.

Gao, D., Mittal, V., 2012. Tumor microenvironment regulates epithelial-mesenchymal transitions in metastasis. Expert. Rev. Anticancer. Ther. 12, 857–859.

Gao, D., Vahdat, L.T., Wong, S., Chang, J.C., Mittal, V., 2012. Microenvironmental regulation of epithelial-mesenchymal transitions in cancer. Cancer Res. 72, 4883–4889.

Hou, J., Wang, D., Zhang, R., Wang, H., 2008. Experimental therapy of hepatoma with artemisinin and its derivatives: in vitro and in vivo activity, chemosensitization, and mechanisms of action. Clin. Cancer Res. 14, 5519–5530.

Ingeson-Carlsson, C., Nilsson, M., 2014. Dual contribution of MAPK and PI3K in epidermal growth factor-induced destabilization of thyroid follicular integrity and invasion of cells into extracellular matrix. Exp. Cell Res. 326, 210–218.

Janzen, D.M., Tiourin, E., Salehi, J.A., Paik, D.Y., Lu, J., Pellegrini, M., Memarzadeh, S., 2015. An apoptosis-enhancing drug overcomes platinum resistance in a tumour-initiating subpopulation of ovarian cancer. Nat. Commun. 6, 7956.

Jayson, G.C., Kohn, E.C., Kitchener, H.C., Ledermann, J.A., 2014. Ovarian cancer. Lancet 384, 1376–1388.

Lai, H.C., Singh, N.P., Sasaki, T., 2013. Development of artemisinin compounds for cancer treatment. Investig. New Drugs 31, 230–246.
Larue, L., Bellacosa, A., 2005. Epithelial-mesenchymal transition in development and cancer: role of phosphatidylinositol 3′ kinase/AKT pathways. Oncogene 24, 7443–7454.
Li, X., Chen, T., Lin, S., Zhao, J., Chen, P., Ba, Q., Guo, H., Liu, Y., Li, J., Chu, R., et al., 2013a. Valeriana jatamansi constituent IVHD-valtrate as a novel therapeutic agent to human ovarian cancer: in vitro and in vivo activities and mechanisms. Curr. Cancer Drug Targets 13, 472–483.
Li, X., Yang, X., Liu, Y., Gong, N., Yao, W., Chen, P., Qin, J., Jin, H., Li, J., Chu, R., et al., 2013b. Japonicone A suppresses growth of Burkitt lymphoma cells through its effect on NF-kappaB. Clin. Cancer Res. 19, 2917–2928.
Li, X., Yao, W., Yuan, Y., Chen, P., Li, B., Li, J., Chu, R., Song, H., Xie, D., Jiang, X., et al., 2015. Targeting of tumour-infiltrating macrophages via CCL2/CCR2 signalling as a therapeutic strategy against hepatocellular carcinoma. Gut http://dx.doi.org/10.1136/gutjnl-2015-310514 (Epub ahead of print).
Miller, L.H., Su, X., 2011. Artemisinin: discovery from the Chinese herbal garden. Cell 146, 855–858.
Mulholland, D.J., Kobayashi, N., Ruscetti, M., Zhi, A., Tran, L.M., Huang, J., Gleave, M., Wu, H., 2012. Pten loss and RAS/MAPK activation cooperate to promote EMT and metastasis initiated from prostate cancer stem/progenitor cells. Cancer Res. 72, 1878–1889.
Naora, H., Montell, D.J., 2005. Ovarian cancer metastasis: integrating insights from disparate model organisms. Nat. Rev. Cancer 5, 355–366.
Njuguna, N.M., Ongarora, D.S., Chibale, K., 2012. Artemisinin derivatives: a patent review (2006–present). Expert Opin. Ther. Pat. 22, 1179–1203.
Romagnoli, R., Baraldi, P.G., Salvador, M.K., Chayah, M., Camacho, M.E., Prencipe, F., Hamel, E., Consolaro, F., Basso, G., Viola, G., 2014. Design, synthesis and biological evaluation of arylcinnamide hybrid derivatives as novel anticancer agents. J Med Chem.]–>Eur. J. Med. Chem. 81, 394–407.
Sadava, D., Phillips, T., Lin, C., Kane, S.E., 2002. Transferrin overcomes drug resistance to artemisinin in human small-cell lung carcinoma cells. Cancer Lett. 179, 151–156.
Saini, K.S., Loi, S., de Azambuja, E., Metzger-Filho, O., Saini, M.L., Ignatiadis, M., Dancey, J.E., Piccart-Gebhart, M.J., 2013. Targeting the PI3K/AKT/mTOR and Raf/MEK/ERK pathways in the treatment of breast cancer. Cancer Treat. Rev. 39, 935–946.
Sale, S., Orsulic, S., 2006. Models of ovarian cancer metastasis: murine models. Drug Discov. Today Dis. Model. 3, 149–154.
Schultze, S.M., Hemmings, B.A., Niessen, M., Tschopp, O., 2012. PI3K/AKT. MAPK and AMPK signalling: protein kinases in glucose homeostasis. Expert Rev. Mol. Med. 14, e1.
Shi, C., Li, H., Yang, Y., Hou, L., 2015. Anti-inflammatory and immunoregulatory functions of artemisinin and its derivatives. Mediat. Inflamm. 435713.
Solomon, V.R., Hu, C., Lee, H., 2010. Design and synthesis of anti-breast cancer agents from 4-piperazinylquinoline: a hybrid pharmacophore approach. Bioorg. Med. Chem. 18, 1563–1572.
Srivastava, V., Lee, H., 2015. Chloroquine-based hybrid molecules as promising novel chemotherapeutic agents. J Pharmacol.]–>Eur. J. Pharmacol. 762, 472–486.
Steyn, J.D., Wiesner, L., du Plessis, L.H., Grobler, A.F., Smith, P.J., Chan, W.C., Haynes, R.K., Kotze, A.F., 2011. Absorption of the novel artemisinin derivatives artemisone and artemiside: potential application of Pheroid technology. J Pharm.]–>Int. J. Pharm. 414, 260–266.
Thiery, J.P., Acloque, H., Huang, R.Y., Nieto, M.A., 2009. Epithelial-mesenchymal transitions in development and disease. Cell 139, 871–890.
Thompson, K.N., Whipple, R.A., Yoon, J.R., Lipsky, M., Charpentier, M.S., Boggs, A.E., Chakrabarti, K.R., Bhandary, L., Hessler, L.K., Martin, S.S., et al., 2015. The combinatorial activation of the PI3K and Ras/MAPK pathways is sufficient for aggressive tumor formation, while individual pathway activation supports cell persistence. Oncotarget 6, 35231–35246.
Torre, L.A., Bray, F., Siegel, R.L., Ferlay, J., Lortet-Tieulent, J., Jemal, A., 2015. Global cancer statistics, 2012. J Clin.]–>CA Cancer J. Clin. 65, 87–108.
Vaughan, S., Coward, J.I., Bast Jr., R.C., Berchuck, A., Berek, J.S., Brenton, J.D., Coukos, G., Crum, C.C., Drapkin, R., Etemadmoghadam, D., et al., 2011. Rethinking ovarian cancer: recommendations for improving outcomes. Nat. Rev. Cancer 11, 719–725.
Xie, L., Zhai, X., Ren, L., Meng, H., Liu, C., Zhu, W., Zhao, Y., 2011. Design, synthesis and antitumor activity of novel artemisinin derivatives using hybrid approach. Chem. Pharm. Bull. 59, 984–990.
Yang, X., Wang, W., Tan, J., Song, D., Li, M., Liu, D., Jing, Y., Zhao, L., 2009. Synthesis of a series of novel dihydroartemisinin derivatives containing a substituted chalcone with greater cytotoxic effects in leukemia cells. Bioorg. Med. Chem. Lett. 19, 4385–4388.
Yap, T.A., Carden, C.P., Kaye, S.B., 2009. Beyond chemotherapy: targeted therapies in ovarian cancer. Nat. Rev. Cancer 9, 167–181.
Zuo, Z.Z., Zhong, H., Cai, T., Bao, Y., Liu, Z.Q., Liu, D., Zhao, L.X., 2015. Design, synthesis and antiproliferative activities of artemisinin derivatives substituted by N-heterocycles. Acta Pharm. Sin. 50, 868–874.